VOLCANIC ASH AND AVIATION SAFETY:
Proceedings of the First International Symposium
on Volcanic Ash and Aviation Safety
U.S. GEOLOGICAL SURVEY BULLETIN 2047

OBSERVATIONS OF THE 1989–90 REDOUBT VOLCANO ERUPTION CLOUDS USING AVHRR SATELLITE IMAGERY

By David J. Schneider *and* William I. Rose

ABSTRACT

The 1989–90 eruptions of Redoubt Volcano, Alaska, generated ash clouds that reached altitudes of as much as 12 km and provided an opportunity to test and refine the use of the advanced very high resolution radiometer (AVHRR) for satellite remote sensing of volcanic eruption clouds. Several aircraft encountered dispersed volcanic clouds, including a Boeing-747 that temporarily lost power from all four engines. Such near-tragic incidents highlighted the need for improved methods of discriminating and tracking volcanic clouds.

Thirty-one AVHRR images from various stages of the Redoubt eruption were examined. In the early, more energetic phases of the eruption, the Redoubt volcanic clouds could be discriminated by a technique that employs an apparent temperature difference between bands 4 and 5 of AVHRR. This method was particularly successful in clouds that were older than 1 hour, demonstrating that slight aging of the cloud during dispersal enhances its discrimination by this method. In the later stages of Redoubt activity, this method fails, probably because of environmental variables associated with the changing character of the eruption. The ash clouds associated with dome collapses that marked the later Redoubt clouds were of small volume and may not have contained as high a proportion of fine ash particles.

Laboratory biconical reflectance measurements were conducted to determine the spectral variability of ash that fell out of the Redoubt clouds. The results show that ash reflectance is controlled more by particle size than by particle composition, but these alone do not explain the variability we observed in the satellite data.

INTRODUCTION

Satellite remote sensing of volcanic clouds is an important tool for scientists and those engaged in mitigating natural hazards. The total ozone mapping spectrometer (TOMS) has been used to measure the SO_2 released by eruptions (Krueger, 1983; Krueger and others, this volume), and multispectral image processing of advanced very high resolution radiometer (AVHRR) data has succeeded in discriminating volcanic clouds from weather clouds (Hanstrum and Watson, 1983; Prata, 1989a; Holasek and Rose, 1991). Perfection of image-processing algorithms and identification of primary physical parameters controlling success of the algorithms could lead to operational use of AVHRR data in reducing dangerous encounters between aircraft and volcanic clouds (Rose, 1987; Casadevall, 1990; Steenblik, 1990) and for monitoring the global dispersion of large atmospheric injections by volcanoes.

This paper attempts to advance satellite-based volcanic-cloud sensing through analysis of AVHRR data collected during the Redoubt eruptions of 1989–90. In particular, it tests a volcanic-cloud-discrimination algorithm developed by Holasek and Rose (1991) for the 1986 eruption of Augustine Volcano. Redoubt and Augustine Volcanoes, located in the Cook Inlet area of Alaska (Kienle, this volume), both erupted during the winter and early spring and have similar chemical compositions.

AVHRR satellite images collected during various stages of the Redoubt eruption were analyzed to test the utility of cloud-discrimination algorithms. In addition, the spectral variability of the Redoubt volcanic clouds were investigated through analysis of biconical reflectance measurements of samples of ash fallout and crushed pumice, glass, and minerals separated from Redoubt Volcano.

AVHRR SENSOR

The AVHRR sensor, aboard the National Oceanic and Aeronautics Administration (NOAA) polar-orbiting weather satellites since 1978, has been used in the study of several eruptions (Kienle and Shaw, 1979; Hanstrum and Watson, 1983; Matson, 1984; Malingreau and Kaswanda, 1986; Glaze and others, 1989; Holasek and Rose, 1991). AVHRR data from NOAA-10 and NOAA-11 were used to study the Redoubt eruptions. This sensor images a 2,800-Ian-wide swath with a spatial resolution of 1.1 km at the nadir. The AVHRR sensor aboard NOAA-10 has four bands: band 1,

visible (0.58–0.68 pm); band 2, near-infrared (0.73–1.10 μm); band 3, mid-infrared (3.55–3.93 pm); and band 4, thermal-infrared (10.3–11.3 μm), whereas the AVHRR sensor aboard NOAA-11 contains the previous bands plus band 5, thermal-infrared (11.5–12.5 μm). Each satellite passes over a point on the ground twice per day, with more frequent coverage occurring at high latitudes where the orbits converge at the poles. The large swath width, frequent coverage, and multispectral capability make the AVHRR sensor a useful instrument for studying volcanic clouds.

THE 1989–90 ERUPTION OF REDOUBT VOLCANO

Redoubt Volcano is an andesitic composite volcano located in the Cook Inlet region of Alaska, approximately 200 km southwest of Anchorage (fig. 1). In mid-December 1989, Redoubt erupted for the first time since 1966. During the next 5 months, there were more than 20 eruptive episodes, which produced ash clouds reaching greater than 12-km altitude (table 1) (Brantley, 1990). Scott and McGimsey (in press) estimate the total tephra-fall volume to be 2×10^7–4×10^7 m^3, dense-rock equivalent, and note that two different tephra types were produced. Pumiceous tephra was generated by magmatically driven explosions on December 14 and 15, and fine-grained lithic-crystal tephra was erupted starting on December 16 and during all later events. The lithic-crystal tephra was generated by two processes: hydrovolcanic explosions dominated from December 16 to 19, and pyroclastic flows, resulting from dome collapse, became an increasingly important process from January 2, 1990, to the end of eruptive activity in April. Pyroclastic flows were the only mechanism generating tephra during the last five eruptive episodes (Scott and McGimsey, in press).

More than 60 percent of Alaska's population lives in the Cook Inlet region. Major oil facilities are also located in this region, and Anchorage is a major hub of air traffic between Asia and Europe. There were four incidents of commercial aircraft encountering volcanic clouds, including one incident in which a Boeing 747 carrying 246 people lost power from all four engines after flying through a cloud (Casadevall, 1990). The aircraft lost more than 4 km of altitude before two engines were restarted at 5.2 km—the remaining engines were restarted at about 4.1 km (Przedpelski and Casadevall, this volume). The aircraft was extensively damaged (Steenblik, 1990), and the incident highlighted the need for new techniques to detect and track volcanic clouds.

MULTISPECTRAL IMAGE PROCESSING OF THE AVHRR IMAGES

More than 30 images of the Redoubt region were collected from the archive at the NOAA National Environmental Satellite Data and Information Service (NESDIS) and from the University of Alaska's Geophysical Institute following the eruption; 11 images are described in detail in this paper (table 2). In several cases, eruptive episodes are recorded in multiple images, providing an opportunity to track the ash clouds from the initial eruption through the dispersion of the volcanic clouds.

Image processing of the AVHRR scenes was conducted using Erdas and Terascan on a Sparc-1+ workstation. Images of the Redoubt region were extracted from the full scene; the thermal channels were calibrated using the procedure of Kidwell (1991); and the images were georeferenced to a common projection. Following the technique of Prata (1989a) and Holasek and Rose (1991), algebraic manipulations were

Table 1. Chronology of the 1989–90 eruption of Redoubt Volcano.

[Modified from Brantley (1990). X, volcanic activity occurred; na, not applicable; ?, volcanic activity uncertain; cont., continuous; fr., from]

Day	Time[1]	Type of volcanic activity: Explosion[2]	Dome collapse	Plume height
December 1989				
14	9:47	X(17)	na	>10 km
15	1:40	X(12)	na	?
	3:48	X(10)	na	?
	10:15	X(40)	na	>12 km
16-18	(Nearly cont. ejection of tephra fr. crater)			<7 km
19	6:30	X(9)	na	>9 km
January 1990				
2	17:48	X(26)	X	>12 km
	19:27	X(61)	X	>12 km
8	10:09	X(15)	X	>12 km
11	10:01	X(5)	?	>9 km
	13:42	X(12)	?	?
16	22:48	X(13)	?	>11 km
February 1990				
15	4:10	X(20)	X	>10 km
21	12:32	X(6)	X	9 km
24	5:05	X(4)	X	9km
28	9:47	X(5)	X	8 km
March 1990				
4	20:39	X(8)	X	12 km
9	9:51	X(10)	X	10 km
14	9:47	X(14)	X	12 km
23	4:04	X(8)	X	>10 km
29	10:33	X(7)	X	?
April 1990				
6	17:23	X(7)	X	9 km
15	14:49	X(8)	X	>10 km
21	18:11	X(4)	X	>8 km

[1] Alaska Standard Time.

[2] Numbers in parentheses indicate duration of explosive activity in minutes, based on seismicity.

Table 2. Satellite images of Redoubt volcanic clouds used in this study.

[LUT (look-up table) represents image channel color rendition in red (R), green (G), and blue (B)]

Date and start time (GMT[1])	Color, LUT R	G	B	Satellite	Cloud type[2]
12/16/89 12:18	4m5	3	4	NOAA-11	1
12/16/89 13:59	4m5	3	4	NOAA-11	1
12/18/89 21:55	4m5	3	4	NOAA-11	1
12/18/89 23:37	4m5	3	4	NOAA-11	1
01/08/90 19:28	4	4	4	NOAA-10	2
01/08/90 23:13	3m4	3	4	NOAA-11	3
02/15/90 13:17	4	4	4	NOAA-11	2
02/15/90 18:26	3m4	2	1	NOAA-10	3
03/23/90 13:25	4	4	4	NOAA-11	2
03/23/90 18:11	3m4	2	1	NOAA-10	3
03/23/90 23:24	3m4	2	1	NOAA-11	3

[1] Greenwich Mean Time. Local time is GMT minus 9 hours.
[2] See text for discussion of cloud types.

performed on AVHRR bands 4 and 5 to enhance the volcanic clouds and distinguish them from weather clouds. Ratios of band 4 to band 5 and differences between band 4 and band 5 were calculated and evaluated. The subtraction process results in an "apparent temperature difference," which we find particularly useful. The term "apparent temperature difference" is defined as the difference between temperature values derived from emitted energy measured at 10.5–11.3 μm (band 4) and 11.5–12.5 μm (band 5). The temperature difference is not real, but rather it is the result of differential emission of energy at these two wavelengths. When the emittance is converted to a temperature value, it produces an apparent temperature difference. An example of the band-4-minus-band-5 operation is shown in figure 2. In figure 2*A–B*, the single-band images are quite similar, and the volcanic plume is not very distinct. The plume is greatly enhanced by the band subtraction operation (fig. 2*C*), which generally produced better results, in terms of plume discrimination, than the ratio operation. When these operations were not successful, or when using data from NOAA-10 (which does not contain band 5), ratios and differences of band 3 and band 4 were calculated.

The results of these mathematical operations were visually evaluated to determine their ability to enhance volcanic clouds. False-color composites were generated on 24-bit graphic monitors by displaying algebraic enhancements along with several of the AVHRR bands in the red, green, and blue image planes of the monitor. False-color composites are helpful in interpreting the extent of the volcanic cloud because data from the individual bands interact to increase enhancement of the cloud. The various band combinations used to produce the false-color composites are shown in table 2.

OBSERVATIONS OF THE AVHRR IMAGES

For the purpose of description and discussion, the Redoubt volcanic clouds shown in the satellite images are divided into three classes that are chosen on the basis of cloud spectral properties, morphology, and size. It is not implied that these cloud types will be produced by eruptions of other volcanoes or that they are the only type that will be produced. The classes include:

Type-I volcanic clouds.--Clouds generated by magmatic explosions during the first week of activity (while there was a nearly continuous ejection of tephra from the crater). These clouds were low (< 7 km) and extended for hundreds of kilometers from the vent. Examples of this cloud type are shown in figure 3.

Type-2 volcanic clouds.--Clouds generated in part by dome collapse and subsequent pyroclastic flows (Scott and McGimsey, in press). These short-duration, discrete eruptive events were imaged within minutes of the onset of eruption. The type-2 clouds are higher (>10–12 km) than type-1 clouds and have a distinctive, circular morphology. Examples of these clouds are shown in figure 4.

Type-3 volcanic clouds.—Dispersed type-2 clouds. These clouds were imaged several hours after the initial eruptive event and show the dispersion of clouds produced by a single eruptive pulse. Examples of these clouds are shown in figure 5.

Although volcanic clouds were discriminated from weather clouds in many cases, no single algorithm was successful in enhancing all three cloud types. For the type-1 clouds, the band-4-minus-band-5 operation of Prata (1989a) and Holasek and Rose (1991) worked to discriminate portions of the volcanic cloud from the weather clouds (fig. 3A–D). This operation was successful for both daytime and nighttime images, but the discrimination is enhanced in the daytime images when band 3 data are included. All of the false-color composites in figure 3 were produced using identical band combinations (table 2), but a dramatic difference can be seen between the nighttime images from December 16 (fig. 3*A–B*) and the daytime images from December 18 (fig. 3C–D). Band 3 of the AVHRR sensor (3.53–3.93 pm) is a hybrid band, measuring thermal emittance at night and a combination of reflectance and emittance during the day. In the nighttime images, the enhanced portion of the volcanic cloud is red, indicating that the enhancement is solely caused by the band-4-minus-band-5 subtraction operation. By contrast, the volcanic cloud in the daytime images is yellow, indicating that the enhancement is a result of both the subtraction operation and high band 3 reflectance of the volcanic cloud with respect to the weather clouds.

The distal portions of two of the type-1 volcanic clouds were enhanced more than the proximal portions (fig. 3A–B). Near the vent, the volcanic cloud is spectrally similar to the weather clouds seen at the bottom of the image—the

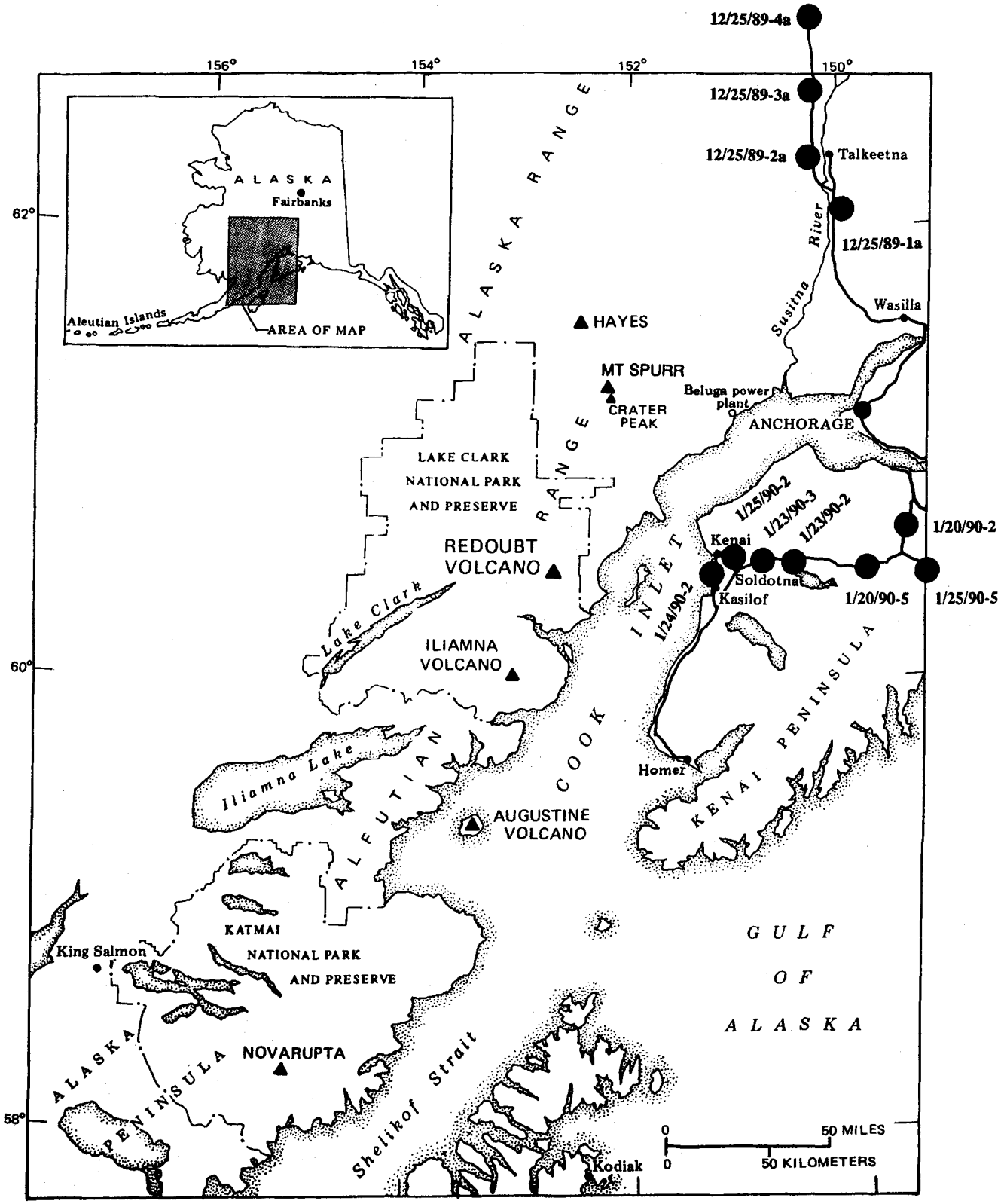

Figure 1. Index map of the Cook Inlet Region of Alaska. Sample locations of the ash spectra shown in figure 6 are indicated by solid circles. Figure modified from Brantley (1990).

subtraction operation is successful once the cloud disperses. Note that, in both cases, the subtraction operation is successful once the cloud has been transported approximately 100 km, or about 1 hour, from the vent. A z-shaped bend in the unenhanced portion of the volcanic cloud (east of Kenai) seen in figure 3A can be seen in figure 3B as an enhanced portion of the volcanic cloud. This image was collected about 1 hour after the previous image (fig. 3A) and shows that the discrimination becomes more distinctive as the volcanic cloud disperses.

In some cases, the effectiveness of the band-4-minus-band-5 operation in discriminating dispersed volcanic clouds is influenced by the underlying surface. Holasek and Rose (1991) found that their algorithm was more successful in discriminating volcanic clouds over water than over land, and effects of the underlying surface are observed in several images from Redoubt. In figure 3A, the discrimination of the volcanic cloud is distinct where the cloud passes over the western Kenai Peninsula and over the water of Prince William Sound, but the cloud is not apparent where it passes over the snow-covered mountains. In figure 3C, the discrimination of the cloud is reduced where it overlies low clouds over land.

Whereas the band-4-minus-band-5 difference was successful in discriminating type-1 volcanic clouds, this operation was not successful with type-2 clouds. These clouds are shown in figure 4 as band-4 thermal images, and they were identified by their anomalously low temperature (220°–230°K), their circular morphology, and their location relative to the vent. An inverted grayscale has been applied to the images in figure 4 so that details of the cold volcanic clouds are discernible.

These images were collected between 7 and 21 minutes after the onset of the eruption, as determined by seismicity (Brantley, 1990), and show that the cloud is detached from the vent, supporting the interpretation of Scott and McGimsey (in press) that these volcanic clouds were generated by

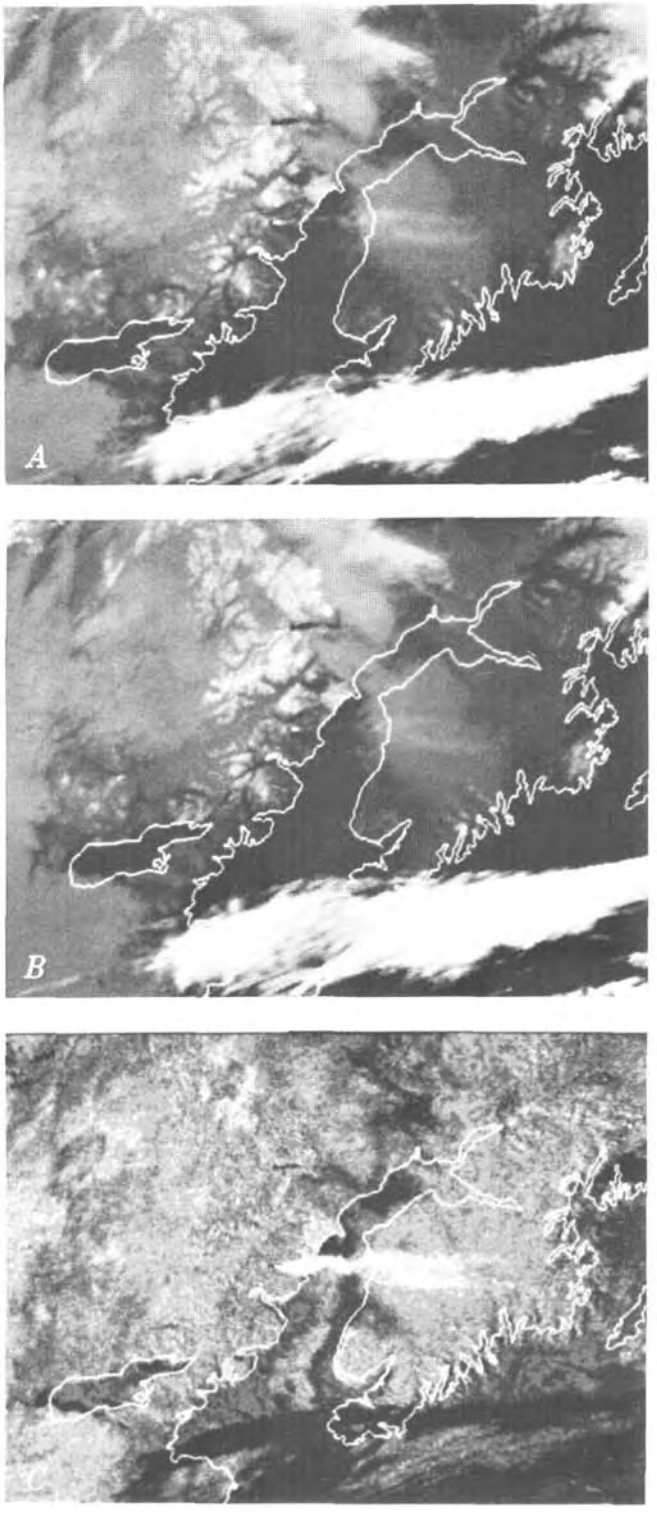

Figure 2 (right). NOAA-I1 AVHRR images demonstrating the discrimination of a volcanic eruption cloud from weather clouds. Image was collected on December 18, 1989, at 23:37 GMT. All images are shown with an inverted grayscale, so that cold objects are bright and warm objects are dark. *A*, AVHRR band-4 image showing an indistinct plume from Redoubt and weather clouds throughout the scene. B, AVHRR band-5 image. *C*, The result of a band-4-minus-band-5 operation. Note that the volcanic plume is a bright feature and that the weather clouds appear gray to black.

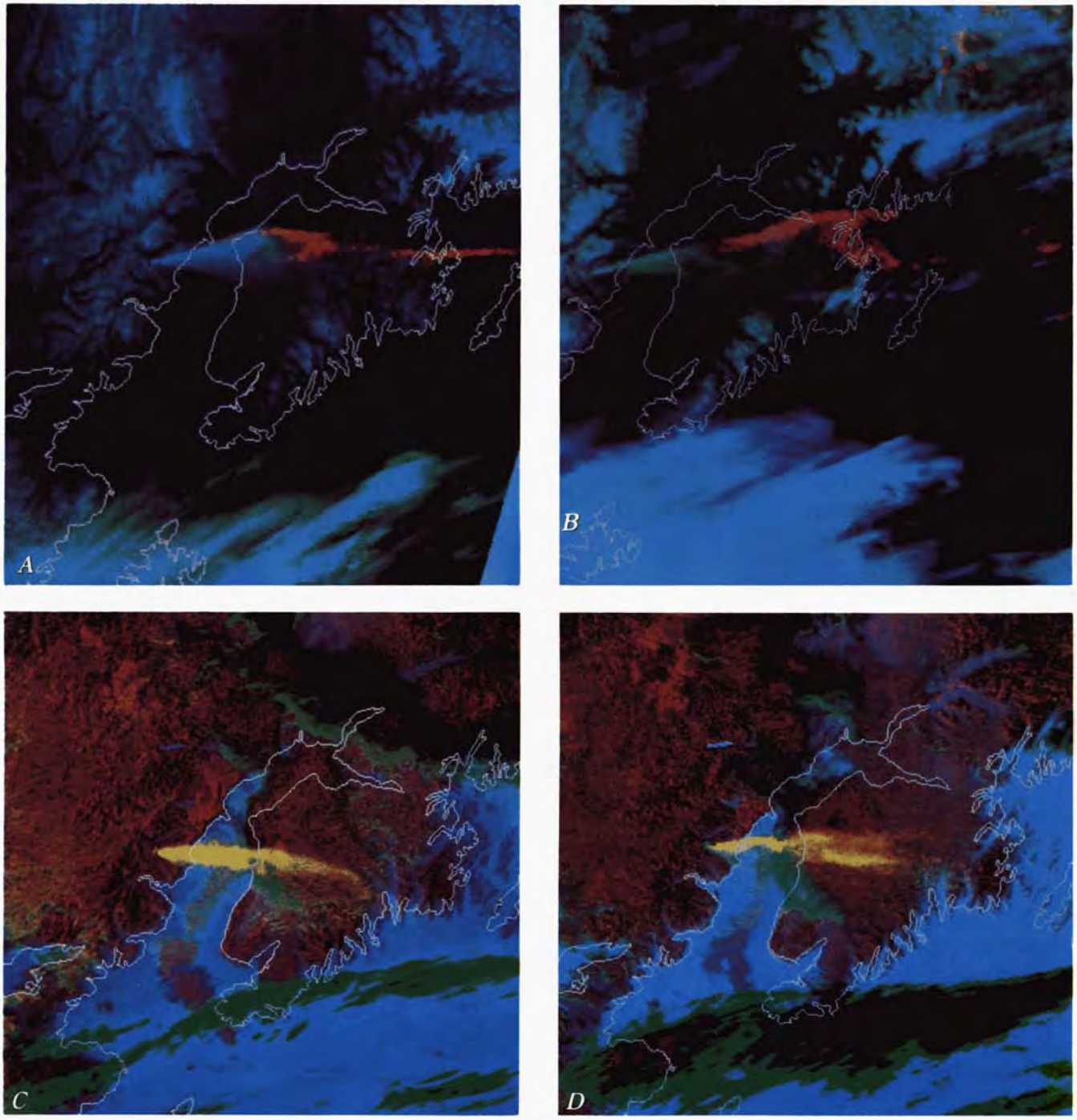

Figure 3. False-color composite AVHRR images of type-1 eruption clouds from Redoubt Volcano. All of the color composites were produced using band 4 minus band 5 in red, band 3 in green, and band 4 in blue. See text for description of cloud types. A, NOAA-11 image collected on December 16, 1989, at 12:18 GMT. B, NOAA-11 image collected on December 16, 1989, at 13:39 GMT. C, NOAA-11 image collected on December 18,1989, at 21:55 GMT. D, NOAA-11 image collected on December 18,1989, at 23:37 GMT.

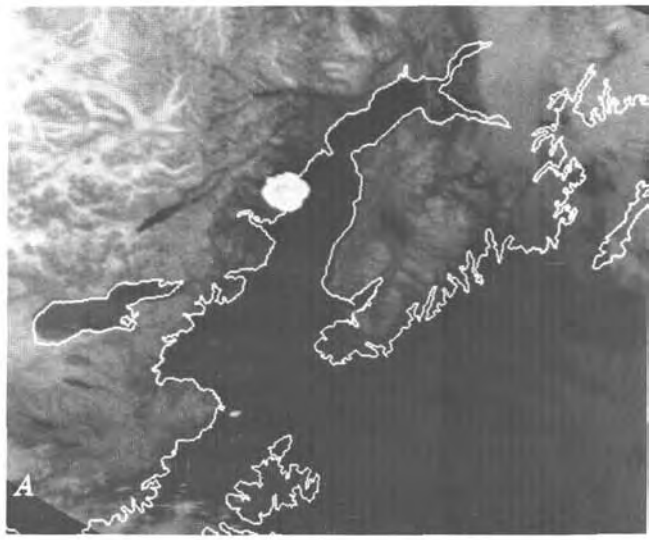

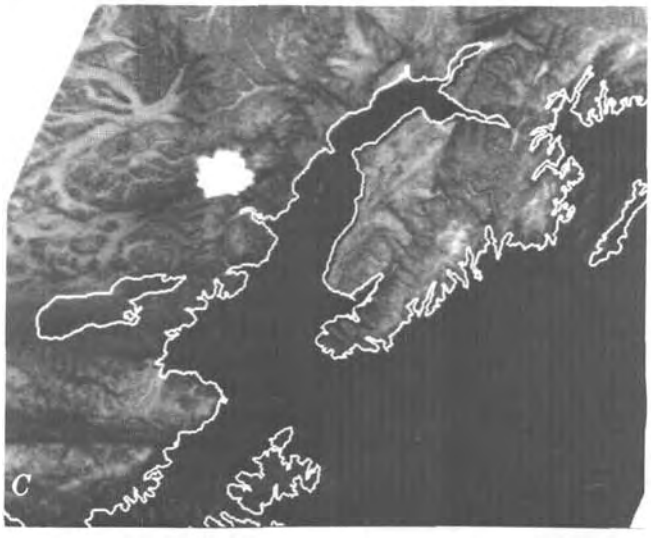

dome collapse and pyroclastic flows. Dispersal of these clouds and transformation into type-3 clouds are monitored in subsequent images, and the observations of these clouds are discussed below.

Even though it appears that the volcanic clouds show variation in cloud-top topography, this cannot be quantified. It is possible to determine cloud-top elevation and topography by relating the temperature of the cloud, as determined by one or more thermal bands of the satellite sensor, with a temperature profile of the atmosphere as determined by radiosonde or other methods. Altitude values for each cloud pixel can be determined in this manner. Whereas this method is useful for tropospheric clouds, it is unsuccessful at higher altitudes due to the temperature inversion that defines the tropopause. All of the type-2 volcanic clouds penetrated the stratosphere, which starts at about 10-km altitude during the Arctic winter, limiting height estimates of clouds to a minimum value and preventing the determination of cloud-top topography.

The frequent coverage of the NOAA satellites provided opportunities to observe the transport and dispersion of the Redoubt volcanic clouds. These dispersed, type-3, volcanic clouds were enhanced by a band-3-minus-band-4 operation. The dispersed volcanic cloud from the January 8, 1990, eruptive episode is seen in figure 5A. This image was collected about 5 hours after the start of the eruption seen in figure 4A and shows a yellow, comma-shaped cloud extending from north of Anchorage to the southern coast of the Kenai Peninsula and a more dilute, hazy cloud extending back toward the vent. The volcanic cloud is shown in yellow, indicating that the enhancement results from a combination of the band-3-minus-band-4 operation and high band-3 reflectance of the volcanic cloud with respect to weather clouds.

Figure 4 (left). Inverted grayscale AVHRR band-4 thermal images of type-2 eruption clouds from Redoubt Volcano. See text for description of cloud types. A, NOAA-10 image collected on January 8, 1990, at 19:28 GMT. B, NOAA-11 image collected on February 15, 1990, at 18:26 GMT. C, NOAA-11 image collected on March 23, 1990, at 13:25 GMT.

Figure 5 (following pages). False-color composite AVHRR images of type-3 eruption clouds from Redoubt Volcano. See text for description of cloud types. All of the color composites, except A, were produced using band 3 minus band 4 in red, band 2 in green, and band 1 in blue. A, NOAA-11 image collected on January 8, 1990, at 23:13 GMT. This color composite was produced using band 3 minus band 4 in red, band 3 in green, and band 4 in blue. B, NOAA-10 image collected on February 15, 1990, at 18:26 GMT. C, NOAA-10 image collected on March 23, 1990, at 18:11 GMT. D, NOAA-11 image collected on March 23, 1990, at 23:24 GMT.

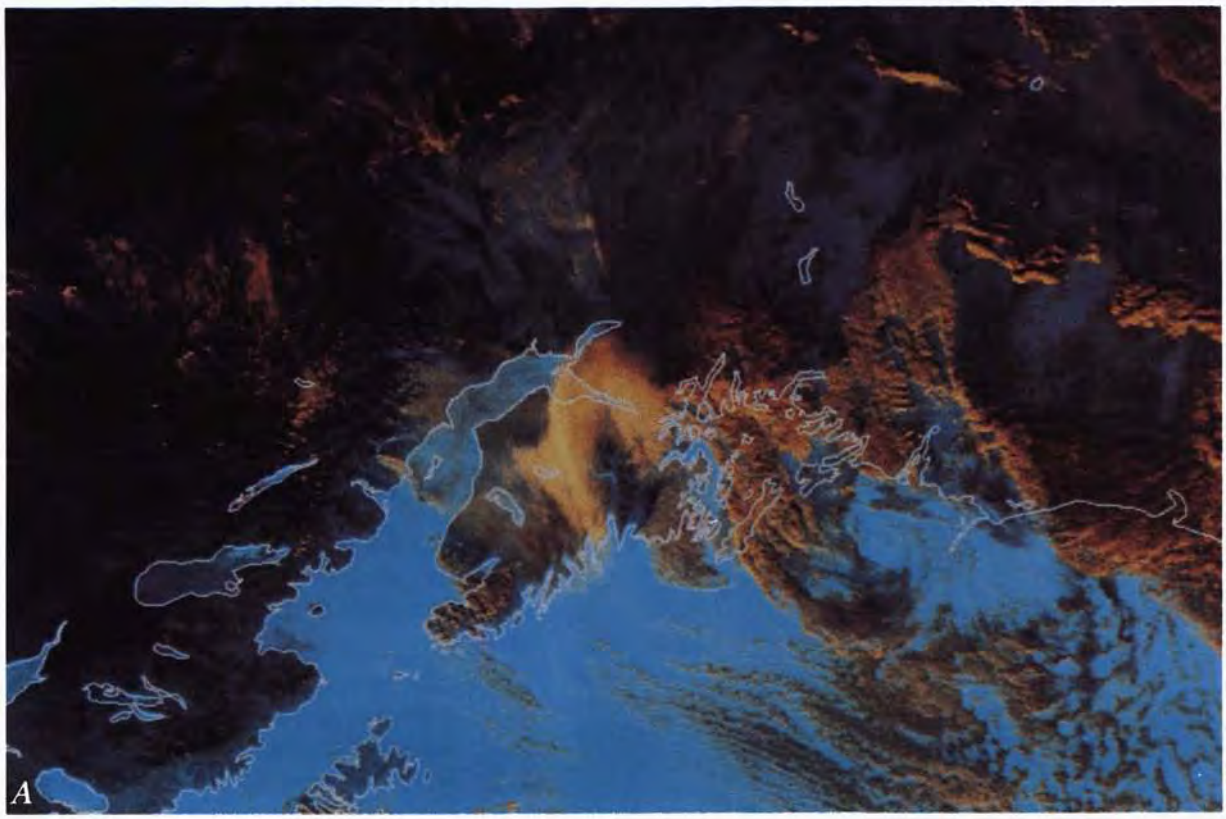
A

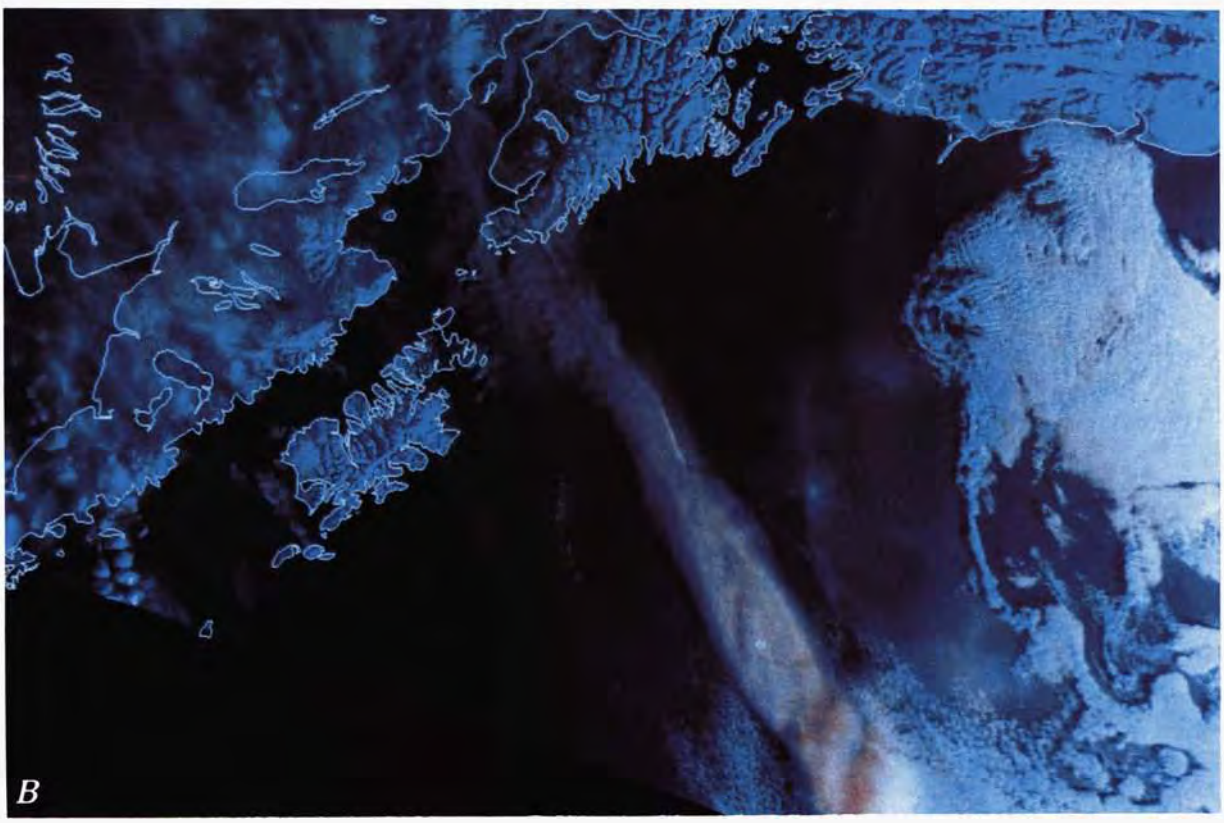
B

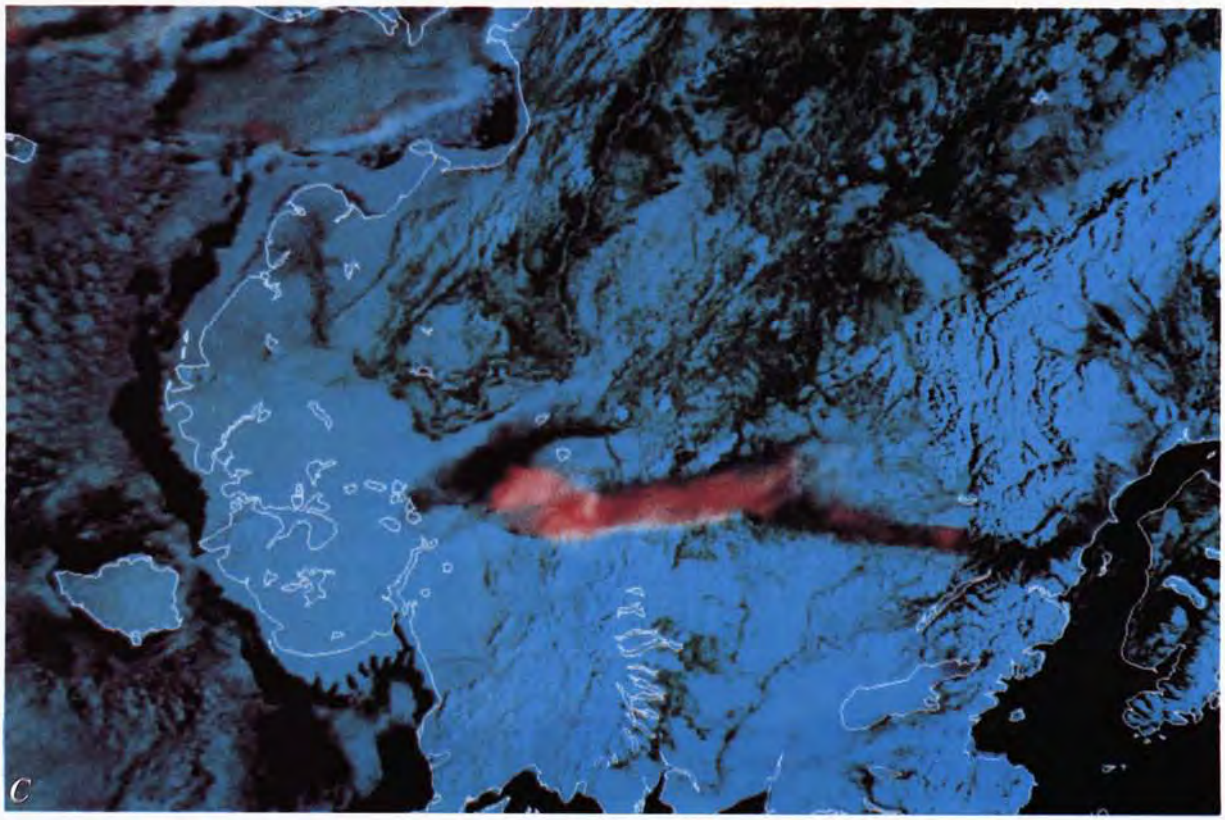
C

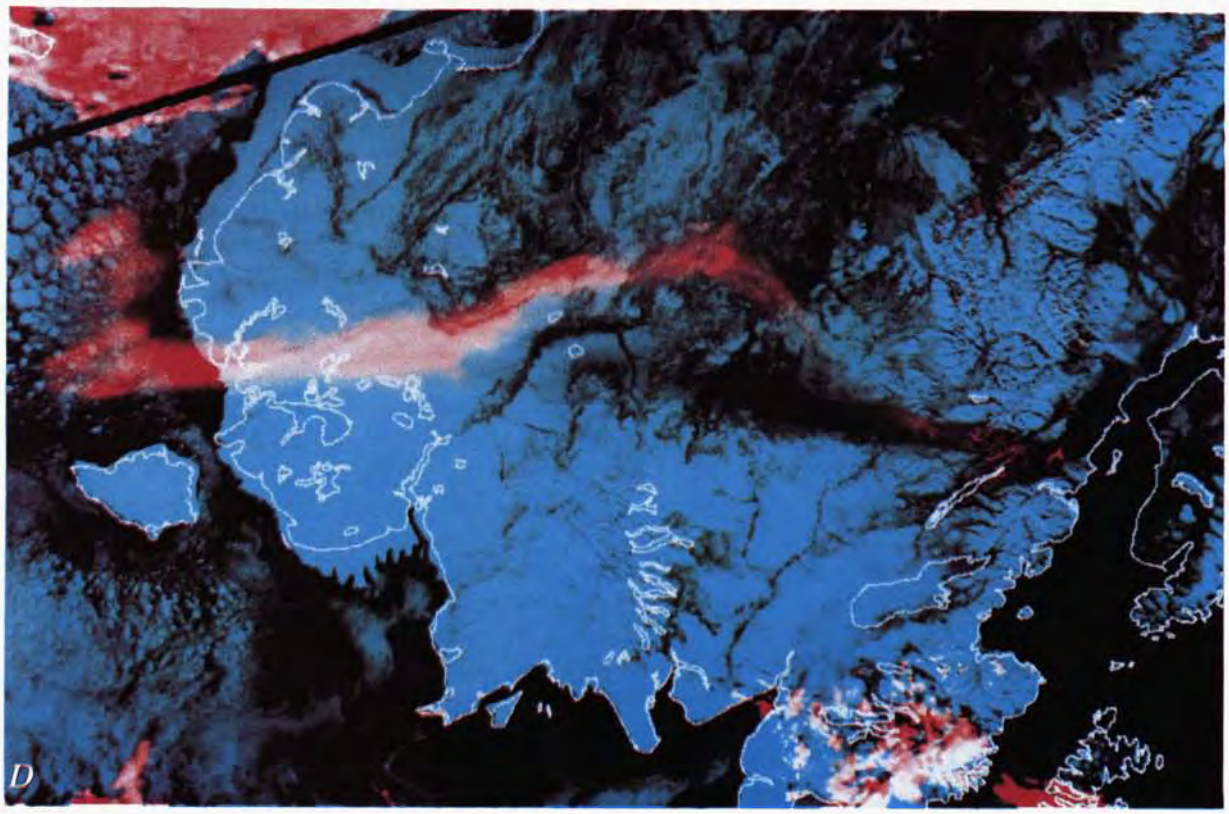
D

The band-4-minus-band-5 operation was not successful in discriminating this cloud, and theories regarding the failure of this operation are included in the discussion.

Another type-3 cloud, from the February 15, 1990, eruptive episode, is seen in figure 5B. The image was collected about 5 hours after the initial eruption seen in figure 4B and consists of a linear, light-red cloud extending from the bottom of the image back toward the volcano, in the upper left of the image. At this time, the cloud front had traveled more than 800 km to the southeast over the Gulf of Alaska. Even though the band-3-minus-band-4 operation was useful in enhancing the volcanic cloud, some of the weather clouds have a similar spectral signal. In this case, manual image interpretation is needed to define the limits of the volcanic cloud. This image was collected by NOAA-10, which contains one thermal band, so it was not possible to attempt the band-4-minus-band-5 operation.

A third type-3 volcanic cloud, from the March 23, 1990, eruption, is seen in two successive images, one NOAA-10 image collected 5 hours after the initial eruption (fig. 5C) and a NOAA-11 image collected 5 hours later (fig. 5D). In figure 5C, the circular volcanic cloud front has traveled about 450 km, and a tail trails back toward the vent. The band-3-minus-band-4 operation was used to enhance the volcanic cloud, but the clarity of the enhancement is diminished by multiple data line dropout along the northern boundary of the volcanic cloud.

In the NOAA-11 image acquired 5 hours later (fig. 5D), the continued dispersal of the volcanic cloud can be seen. The cloud front now extends for more than 825 km, from near the vent to the Bering Sea. Once again, the band-3-minus-band-4 operation helped to enhance the volcanic cloud, but it did not discriminate it from the weather clouds along the top of the scene. The northward bend in the cloud seen in this image is also apparent in the previous image (fig. 5C) and may be due to wind shear. Ash fallout from this eruption is visible as a dark band that trends west for about 300 km and is correlated to the distribution of ash on the ground as mapped by Scott and McGimsey (in press).

REFLECTANCE SPECTRA OF VOLCANIC ASH

The reflectance properties of 19 volcanic ash samples from Redoubt were investigated to see how they varied with transport, and how they varied throughout the eruption. These samples were collected by personnel of the Alaska Volcano Observatory in the weeks to months following the eruption. All of the ash samples used in this study were collected from snowpits throughout Alaska (fig. 1) and were correlated by Scott and McGimsey (in press) to eruptive events by their stratigraphic position. The ash was separated from the snow by melting and filtration, eliminating any sulfuric-acid coatings that may have been present.

To aid in interpretation of the ash reflectance spectra, glass and mineral separates were also prepared. Pumice fragments from the December 15, 1989, eruptive event were crushed mechanically, and glass and crystals were separated using heavy-liquid-separation techniques. The pumice, crystal, and glass separates were sieved to produce a 0.25-mm to 0.088-mm sample, and subsets of these samples were crushed to produce a sample of less than 0.088 mm. This was done to reflect the reduction in grain size and the fractionation of the crystals with respect to glass that occurs as volcanic clouds age and are transported. The crystal separates were composed primarily of plagioclase, with lesser amounts of hornblende and pyroxene.

Laboratory biconical reflectance measurements were conducted on the ash samples and mineral separates by the Jet Propulsion Laboratory (JPL) (J. Crisp, JPL, oral commun., 1991). Although the AVHRR sensor measures emitted energy, reflectance measurements can be related to emittance, which is difficult to measure in the laboratory (Bartholomew and others, 1989). Kirkoff's law states that, for a given temperature and wavelength, emittance and reflectance are complementary. This law only applies to solid objects because scattering is ignored. Although this is a major simplification, we use it to correlate reflectance measurements to the emittance recorded by the satellite sensor.

Biconical reflectance spectra of ash fallout from eruptions on December 15, 1989, December 16, 1989, and from January 8, 1990, are shown in figure 6A–C. These reflectance spectra are typical of the 19 ash samples that were measured and show two reflectance peaks of interest to this study. The first peak extends from 3 μm to 5 μm and contains AVHRR band 3, whereas the second peak extends from 8 pm to 12 μm and contains AVHRR bands 4 and 5. In the region containing AVHRR band 3, the reflectance varies by 10–15 percent between eruptive episodes, and, for the December 15, 1989, event, the reflectance increases by 20 percent as the distance from the vent increases. In contrast, all of the samples show a broad similarity in reflectance in the region containing AVHRR bands 4 and 5, except for the sample suite from the December 15, 1989, event, where the reflectance increases by 1–2 percent with increasing distance from the vent.

The reflectance spectra of the pumice and the glass and crystal separates are shown in figure 7A–B. All of the coarse-grained samples (fig. 7A) show a reflectance peak at 9 pm. The reflectance at 9 μm is less prominent for the crystal separate and the pumice sample, and the glass separate has a smaller reflectance peak at 11.5 pm. The fine-grained samples (fig. 7B) show a much-diminished reflectance peak at 9 μm for the glass separate and none for the pumice sample and crystal separate. The peak at 11.5 μm is most prominent for the glass sample, but the pumice and crystal separates also have a broad peak in this region. These spectra show that reflectance is influenced more by particle size than by particle composition.

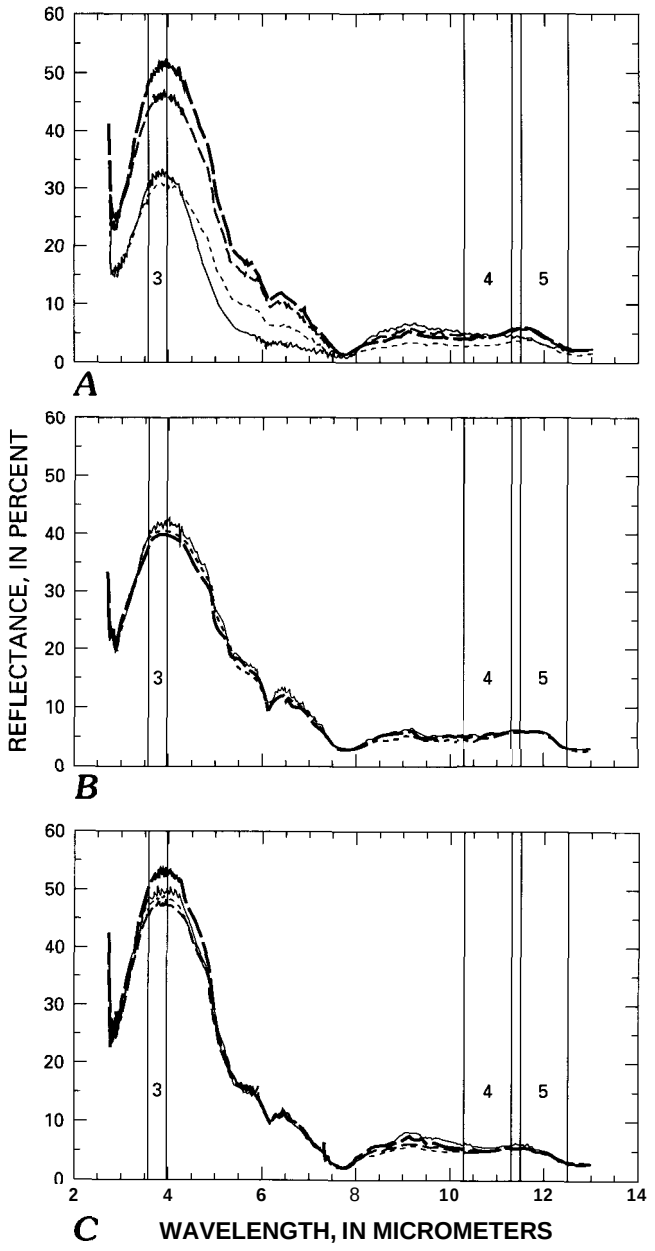

Figure 6. Biconical reflectance plot of ash samples from three eruptions of Redoubt Volcano. The band widths of AVHRR bands 3, 4, and 5 are indicated. Sample locations are shown in figure 1. *A*, Four ash samples from the December 15, 1989, eruption. B, Three ash samples from the December 16, 1989, eruption. *C*, Four ash samples from the January 8, 1990, eruption.

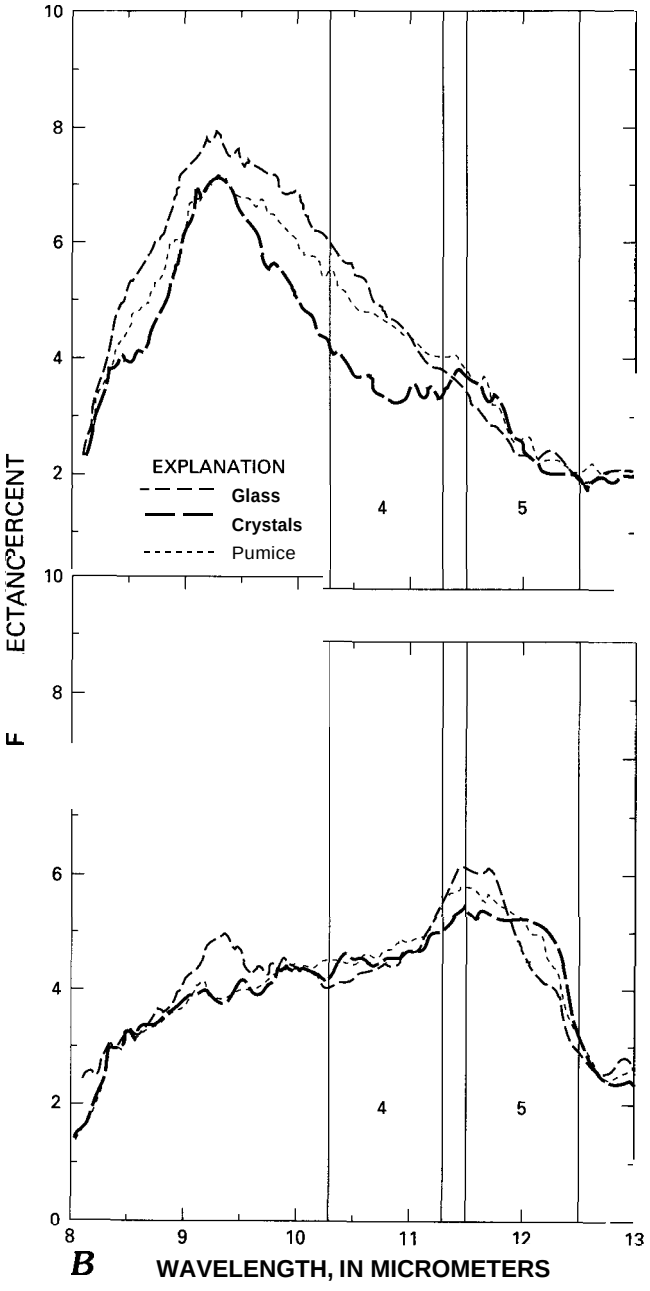

Figure 7. Biconical reflectance plots of pumice, glass, and crystal separates from Redoubt Volcano. *A*, Sieved 0.25–0.88-mm samples. *B*, Sieved > 0.088-mm samples. The band widths of AVHRR bands 4 and 5 are indicated.

DISCUSSION

The spectral discrimination of volcanic clouds is complicated by dynamic processes that occur during the eruption, transport and dispersion of the cloud—these processes may prevent the use of a single image-processing algorithm for use on all volcanic clouds. Previous researchers (Prata, 1989a, 1989b; Holasek and Rose, 1991) have utilized differences and ratios of AVHRR bands 4 and 5 to discriminate volcanic clouds from weather clouds, but these operations were only partially successful at Redoubt. It has been shown that the band-4-minus-band-5 subtraction operation produces positive apparent temperature differences (AT) for weather clouds and negative apparent temperature differences for volcanic clouds (Yamanouchi and others, 1987; Prata, 1989b). However, positive apparent AT's can occur for volcanic clouds if the cloud contains a large amount of water or if the particle size is large (Prata, 1989b).

The early eruptions of the Redoubt series (type-1 clouds) more closely resemble the kinds of ash clouds that are likely to be of most concern to aviation safety than do the later ones. Two important features of these early clouds are the success of the discrimination algorithm based on apparent AT determined from bands 4 and 5 and the indication that, for success of the algorithm, the cloud must have aged (dispersed freely in the atmosphere) for 1 hour or more. Several observations point to the role of fine silicate particles in explaining these phenomena. Biconical reflectance data suggest that fine particle size may enhance the 4-minus-5 effect, and magmatic explosions resulting from explosive vesiculation may be more likely to produce fine ash than dome collapse. Aging of a volcanic cloud will result in decreasing the grain size of suspended ash because fallout will remove larger particles, and it will also tend to reduce the water or ice in the cloud, thereby enhancing the relative importance of the fine ash particles. Because the largest and most broadly hazardous ash clouds are magmatic (and are likely to generate drifting ash clouds that contain significant concentrations of fine ash) these observations are likely to be of general applicability.

The band-4-minus-band-5 operation produced positive AT's for both volcanic and weather clouds in images of type-2 volcanic clouds from Redoubt, which were collected within 30 minutes of the start of the eruption. These volcanic clouds probably contained large amounts of water, due to the entrainment of moist air from the lower atmosphere, and were identified in band-4 thermal images by their proximity to Redoubt, their circular morphology, and cold temperature (fig. 4*A–C*). Volcanic clouds of this type could be confused with convective weather clouds, but this is unlikely in winter Arctic images. In two of the images (fig. 3A–B) of type-1 clouds, the band-4-minus-band-5 operation produced positive AT's for the proximal portion of the cloud and negative AT's for distal portions of the cloud. The region of negative AT is shown in red in figure ***3A–B.*** We attribute the change in the spectral signature of this volcanic cloud to a decrease in particle size and water content during transport. Analysis of wind-speed data for this eruption indicates that the transition from positive to negative difference values in the volcanic cloud took about 1 hour.

Type-3 volcanic clouds were difficult to discriminate, perhaps due to their relatively small volume and the dispersion and sedimentation of ash that occurred before they were imaged. Whereas many volcanic clouds can be discriminated using the band-4-minus-band-5 operation, the concentration of ash required to produce a detectable signal is unknown. Another factor that affects the subtraction operation is particle size. The type-3 clouds may have contained fewer fine particles than the type-1 clouds because they were produced as part of a dome collapse, rather than from a purely explosive, volatile, effervescent mechanism, thus reducing the ash signal.

The band-3-minus-band-4 operation was useful in enhancing type-3 clouds, but it did not discriminate them from weather clouds. This operation was more successful during the daytime hours, when band-3 backscatter is important, than at night, when this band has a larger thermal component. Although this is a useful operation, it is difficult to make general observations regarding its success because the reflectance is dependent on a number of factors, including particle size, shape and abundance, sun azimuth and elevation, and the location of the cloud and the satellite relative to the sun. However, this operation, used in conjunction with observations of cloud morphology, can be used to interpret the extent of probable volcanic clouds.

The use of ash fallout reflectance measurements as "ground truth" for interpreting satellite imagery has several shortcomings. One fundamental problem is that the reflectance measurements were made on ash fallout, which by definition is not what is in the volcanic cloud. Very fine particles are probably the most important, yet their collection is difficult because their fallout may be too light to be distinguished on the ground, and the particles fall out long distances from the vent over very broad areas. Another problem lies in relating the reflectance measurements to the emittance recorded by the sensor. Volcanic clouds are heterogeneous assemblages of particles and gases; therefore, subtracting the reflectance measurements from a black body of the appropriate temperature is a poor approximation. Additional work needs to be done to determine the most effective way of using reflectance measurements of ash fallout as "ground truth" for image interpretation.

In spite of these difficulties, the mineral separate spectra show that reflectance is controlled more by particle size than by the particle composition. In a volcanic cloud, this would imply that the discrimination of distal clouds would be controlled more by the reduction in the size distribution of the particle with transport than by the increase in the proportions of volcanic glass in the cloud due to eolian fractionation. Although the exact relationship of reflectance to

emittance is unknown, the effects of particle size, particle shape, and particle composition would probably be enhanced for suspended particles. In this case, the complex shape of glass particles compared to crystals may have an important effect on the emittance of volcanic clouds.

This study has shown that the discrimination of volcanic clouds using AVHRR imagery is more complex than previously thought and has identified several parameters that contribute to this complexity. These include cloud water content and particle size, concentration, and composition. Additional factors not included in this study include the role of acid aerosols (Prata, 1989a) and sensor viewing geometry. The relative importance of each of these parameters can be investigated in laboratory experiments utilizing an imaging radiometer to observe simulated volcanic clouds. Images can be collected at the same wavelength intervals as the AVHRR sensor, and image-processing operations similar to the ones described in this paper can be conducted. Results of the laboratory studies can be used to guide future work on thermal imaging and particle and gas sampling of actual volcanic clouds.

CONCLUSIONS

Volcanic clouds of a variety of types and scales were observed and mapped by AVHRR images during the Redoubt eruptions of 1989–90. These examples broaden the experience on volcanic cloud tracking and discrimination using multispectral image-processing techniques and provide insight on additional work that needs to be conducted.

A major conclusion of this paper is that volcanic clouds have natural variability that is reflected in satellite images and that affects the methods used to discriminate and map their dispersion. This variability is magnified for activity like that of Redoubt Volcano, which changed eruptive mechanism during its period of activity. Most ash-producing eruptions from other volcanoes, particularly the larger ones, are more likely to resemble the early (type-1) clouds of Redoubt. This is encouraging because the simple method of discrimination of volcanic clouds using apparent temperature differences between AVHRR bands 4 and 5 works well on type-1 clouds; therefore, the simplest methodology is likely to be useful in many of the most serious cases. Discrimination of volcanic clouds using the band-4-minus-band-5 operation is difficult or impossible for very young clouds with high water content and (or) a large particle size, but it is very useful for drifting volcanic clouds. A major uncertainty of this method is the particle concentration required to produce a measurable signal.

Ash reflectance is controlled more by particle size than by particle composition. The fractionation of glass and crystals in a volcanic cloud are not likely to produce reflectance and emittance differences on their own, but fractionation will operate in conjunction with the proportional increase of fine particles as the cloud disperses. Laboratory reflectance measurements are inadequate to explain the spectral variability observed in the imagery of the Redoubt volcanic clouds. Emittance measurements need to be made of simulated volcanic clouds in the laboratory and in situ measurements and particle sampling need to be conducted on actual volcanic clouds to provide "ground truth" for interpretation of satellite imagery.

ACKNOWLEDGMENTS

We would like to thank the following people and organizations for their cooperation and support for this study. Mike Matson of NOAA/NESDIS provided most of the AVHRR data, and Ken Dean of the University of Alaska's Geophysical Institute provided several AVHRR scenes. Joy Crisp of the Jet Propulsion Lab made the ash reflectance measurements, and the Alaska Volcano Observatory furnished field support. This study was funded in part by NSF Grant 91-17726 and NASA Grant 1442-VC1P-011-91.

REFERENCES CITED

Bartholomew, M.J., Kahle, A.B., and Hoover, G., 1989, Infrared spectroscopy (2.3–20 μm) for the geological interpretation of remotely sensed multispectral infrared data: International Journal of Remote Sensing, v. 10, p. 529–544.

Brantley, S.R., ed., 1990, The eruption of Redoubt Volcano, Alaska, December 14,1989–August 31, 1990: U.S. Geological Survey Circular 1061, 33 p.

Casadevall, T.J., 1990, The 1989–90 eruption of Redoubt Volcano, Alaska, impacts on aircraft operations in the vicinity of Anchorage [abs.]: Eos, Transactions, American Geophysical Union, v. 71, p. 1701.

Glaze, L.S., Francis, P.W., Self, S., and Rothery, D.A., 1989, The 16 September 1986 eruption of Lascar Volcano, north Chile, satellite investigations: Bulletin of Volcanology, v. 51, p. 911–923.

Hanstrum, B.N., and Watson, A.S., 1983, A case study of two eruptions of Mount Galunggung and an investigation of volcanic cloud characteristics using remote sensing techniques: Australian Meteorological Magazine, v. 31, p.171–177.

Holasek, R.E., and Rose, W.I., 1991, Anatomy of 1986 Augustine Volcano eruptions as revealed by digital AVHRR satellite imagery: Bulletin of Volcanology, v. 53, p. 420–435.

Kidwell, K.B., ed., 1991, National Oceanic and Atmospheric Administration Polar Orbiter Data Users Guide: Washington, D.C., National Oceanic and Atmospheric Administration/National Environmental Satellite Data and Information Service, 294 p.

Kienle, J., and Shaw, G.E., 1979, Plume dynamics, thermal energy and long-distance transport of Vulcanian eruption clouds from Augustine Volcano, Alaska: Journal of Volcanology and Geothermal Research, v. 6, p. 139–164.

Krueger, A.J., 1983, Sighting of the El Chichón sulfur dioxide clouds with the NIMBUS 7 total ozone mapping spectrometer: Science, v. 220, p. 1377–1379.

Malingreau, J.P., and Kaswanda, 1986, Monitoring volcanic eruptions in Indonesia using weather satellite data: The Colo eruption of July 28, 1983: Journal of Volcanology and Geothermal Research, v. 27, p. 179–194.

Matson, M., 1984, The 1982 El Chichón Volcano eruptions—A satellite perspective: Journal of Volcanology and Geothermal Research, v. 23, p. 1–10.

Prata, A.J., 1989a, Observations of volcanic ash clouds in the 10–12 pm window using AVHRR/2 data: International Journal of Remote Sensing, v. 10, p. 751–761.

———1989b, Infrared radiative transfer calculations for volcanic ash clouds: Geophysical Research Letters, v. 16, p. 1293–1296.

Rose, W.I., 1987, Interaction of aircraft and explosive eruption clouds: A volcanologist's perspective: American Institute of Aeronautics and Astronautics Journal, v. 25, p. 52–58.

Steenblik, J.W., 1990, Volcanic ash: A rain of terra: Air Line Pilot, v. 59, p. 9–15, p. 56.

Salisbury, J.W., and Walter, L.S., 1989, Thermal infrared (2.5–13.5 pm) spectroscopic remote sensing of igneous rock types on particulate planetary surfaces: Journal of Geophysical Research, v. 94, p. 9192–9202.

Scott, W.E., and McGimsey, R.G., in press, Character, mass, distribution, and origin of tephra-fall deposits of the 1989–90 eruption of Redoubt Volcano, south-central Alaska: Journal of Volcanology and Geothermal Research.

Yamanouchi, T., Suzuki, K., and Kawaguchi, S., 1987, Detection of clouds in Antarctica from infrared multispectral data of AVHRR: Journal of the Meteorological Society of Japan, v. 65, p. 949–961.